

Fluorescence measurements are carried out after 2 days of equilibrium at 25 °C.

This compound forms a face-to-face excimer<sup>7</sup> and gives excimer emission ( $F_2$ ) at 470 nm and monomer emission ( $F_1$ ) at 390 nm.

In this experiment, we plotted the value of  $F_2/F_1$  as a function of SDS concentration and also found a sharp break at 70 mM of SDS in good agreement with the one determined by using ANS (Figure 2).

## References

(1) S. K. Omar, J. S. Anthony, *Molecular Photochem.*, **8**,

399 (1977).

(2) E. J. R. Sudholter and J. B. F. N. Engberts, *J. Phys. Chem.*, **82**, 1854 (1979).

(3) K. S. Birdi, T. Krag and J. Clausen, *J. Colloid Interface Sci.*, **62**, 562 (1977).

(4) P. Ekwall and L. Mandell, *J. Colloid Interface Sci.*, **35**, 519 (1971).

(5) P. Mukerjee and K. J. Mysels, Nat. Standard Ref. Data Service of the National Bureau of Standards. No. 36, 15 (1971).

(6) A. Datyner, *J. Colloid Interface Sci.*, **65**, 527 (1978).

(7) T. Forster, *Angew. Chem. Int. Ed. Engl.*, **8**, 333 (1969).

## Thermal Unimolecular Decomposition Reactions of Ethyl Bromide at 724.5–755.1° K

Tae Joon Park and K. H. Jung

*Department of Chemistry, Korea Advanced Institute of Science, Seoul 131, Korea (Received March 6, 1980)*

The thermal decomposition reaction of ethyl bromide was studied in the temperature range of 724.5–755.1°K. Pressure dependence of the reaction was observed in its fall-off region. A theoretical evaluation of the rate constants was carried out adopting RRKM formulation in the region and was compared with the experimental observation. The validity of theory was also reevaluated by using the observed results. The observed activation energy in this study and Arrhenius A-factor were 51.7 kcal/mole and  $10^{12.5}$ , respectively. The small A-factor in the study was discussed in terms of the formation of a tight activated complex and the molecular elimination as a prevalent reaction mode.

## Introduction

The kinetics for the decomposition of ethyl bromide is known to be first-order and mechanism consisted of simple homogeneous molecular splitting and radical chain reaction which can be inhibited by various inhibitors. However, the detailed mechanism of radical reaction is not well established<sup>1-4</sup>.

Fugassi and Daniels<sup>1</sup> have proposed the non-chain radical reaction as the primary decomposition in which ethyl bromide is splitted into ethyl radical and bromine atom. But this suggestion was not fully supported by other workers<sup>2</sup>. It has been also suggested by Goldberg and Daniels<sup>3</sup> that the decomposition is composed of two different types of reactions. They have found the radical chain reaction was catalyzed by the wall and unimolecular splitting was occurred during the induction period which was not detected at temperatures above 400°C. And the overall decomposition exhibited the first-order behavior by the inhibitor even after the induction period. Nevertheless, the disagreements between workers and difficulties of precise product analyses in earlier works are greater than would normally be expected and thus a reinvestigation of this system, coupled with a theoretical treatment, would appear in order. Since spectroscopic data on this system are available the dissociation

of ethyl bromide lends itself to a fairly detailed analysis in terms of the quantum statistical RRKM theory<sup>5</sup> of unimolecular reactions and this forms the objective of the present study.

## Experimental

**Materials.** Ethyl bromide, obtained from Eastmann Kodak Co., was purified several times by fractional distillation and low boiling trap-to-trap distillation until zero detection of impurities by GC. Ethylene stated purity of 99.5%, product of Matheson Co., was purified by the same technique as ethyl bromide. Carbon dioxide state purity of 99.995%, Matheson research grade, was used as a filling gas in the high pressure region without further purification.

**Apparatus.** The reaction system in this study was a static system connected to a standard vacuum line for gas handling and pressure measurement. The reaction vessel was constructed from a total volume 43.5 ml silica tubing with 2.5×6 cm dimension and was heated in an air furnace. The temperature gradient of the reaction section was maximum  $\pm 2^\circ\text{C}$  over entire temperature range, i.e., 200–700°C, and was calibrated against Leeds and Northrup 8686 potentiometer. Feedback temperature control was carried out by use of Love controller Model 51 on-off type with chromel-alumel K type thermocouple as a detection

probe.

**Procedure.** To provide minimum dead time of reaction, the sudden expansion of measured reactant samples from 1 to 60 torr into the reaction vessel was followed right after trapping the sample in 14 ml sampling vessel. Reaction times were varied from 10 to 20 min depending on the reaction temperature, *i.e.*, 10 min at both 744.5 and 755.1 °K, and 20 min at 724.5 °K. The measurement of reaction time was done manually using a stopwatch. The completion of reaction was performed by trapping reaction products in the sampling vessel back. And analyses of products were followed by injecting these products into GC *via* 6-port Valco gas sampling valve.

**Analysis.** Ethyl bromide and ethylene were analyzed using a home made GC equipped with a hydrogen flame ionization detector (FID). A typical column used in this study was 3 m × 1/8" S.S. Chromosorb century series 108 column. Detector sensitivities and retention times of each product and the reactant were obtained with use of authentic samples. Hydrogen bromide while certainly major products could not determined since FID prevents specific analysis for this compound.

### Theoretical Consideration

According to RRKM theory, the observable unimolecular rate constant expression is given by eq. 1.

$$k_{\text{uni}} = \frac{kT}{h} \frac{P_1^\ddagger}{P_1 P_2} e^{-E_c/kT} \int_{E^\ddagger}^{\infty} \frac{\sum_{E^\ddagger} P(E^\ddagger_{VR}) e^{-E^\ddagger/kT}}{1 + k_{EJ}/Z} \frac{dE^\ddagger}{kT} \quad (1)$$

In the expression,  $P_1^\ddagger$ ,  $P_1$ , and  $P_2$  represent the rotational partition function for the activated complex, the rotational and the vibrational partition functions for the molecule, respectively.  $Z$  is collision frequency which can be calculated from simple collision theory.  $E_c$  and  $E^\ddagger$  are critical and non-fixed energy, respectively.  $\int$

$$\frac{k_{\text{uni}}}{k_\infty} = \frac{1}{P^\ddagger (kT)^{r+1/2} \Gamma(1+r/2)} \int_0^{\infty} \frac{\sum_{E^\ddagger} P(E^\ddagger_{VR}) (E^\ddagger - E_c)^{r+1/2} e^{-E_c/kT}}{1 + B_1 \frac{\sum_{E^\ddagger} P(E^\ddagger_{VR}) (E^\ddagger - E_c)^{r+1/2}}{(E_c + aE_z)^{r-1} F_W}} \frac{dE^\ddagger}{kT} \quad (6)$$

with  $B_1$  given by

$$B_1 = \frac{\sigma_1^\ddagger}{\sigma_1} \frac{P_R^\ddagger}{h} \frac{\Gamma(s) \pi^s (h\nu_i)}{(kT)^{r+1/2} \Gamma(1+r/2)} \frac{1}{z} \quad (7)$$

The geometrical parameters for the molecule and the complex for these computations are given in Table 1. Input data for the RRKM calculation are given in Table 2, and Table 3 shows the vibrational frequencies for the molecule and the complex.

In order to carry out the integration in eq. 6 in terms of the reduced energy  $x$ , the equation may be readily cast into form

$$\frac{k_{\text{uni}}}{k_\infty} = A_1 \sum_{n=1}^3 \int_0^{\infty} \frac{G_n(x) e^{-(E_c + x)/kT}}{1 + (A_2/P) [G_n(x)/H(x)] F_W} dx \quad (8)$$

where

$$G_1(x) = \frac{\Gamma(\alpha^\ddagger + 1) \prod_{i=1}^s h\nu_i x^{\alpha^\ddagger/2}}{\Gamma(1+r/2) (E_c^\ddagger)^\alpha S^\ddagger}, \quad 0 \leq x \leq \theta \quad \int$$

$\sum_{E^\ddagger} P(E^\ddagger_{VR})$  is the total sum of energy eigenstates of the active degrees of freedom of the activated complex at energy  $E^\ddagger_{VR}$ . The microscopic rate constant<sup>5</sup>,  $k_{EJ}$  is given by eq. 2.

$$k_{EJ} = \frac{\sigma_1}{\sigma_1^\ddagger} \frac{1}{h} \frac{\sum_{E^\ddagger} P(E^\ddagger_{VR})}{N^*(E_V) F_W} \quad (2)$$

In eq. 2,  $\sigma_1$  and  $\sigma_1^\ddagger$  are the symmetry numbers of the molecule and the complex, respectively, and  $N^*(E_V)$  is the density of the vibrational energy states of the molecule at energy  $E_V = E_c + E^\ddagger$ . The quantity  $F_W$  in eq. 2 represents a centrifugal correction factor, originally introduced by Marcus<sup>8</sup> as a constant to allow for the contributions of the adiabatic rotations. Among various refinements<sup>7,10</sup>, Waage and Rabinovitch's derivation<sup>8</sup> has shown better agreements with experimental observations and has given by

$$F_W = \frac{1}{1 + (s-1) [(I^\ddagger/I) - 1] kT/(E_c + aE_z)} \quad (3)$$

where  $E_z$  is the zero point energy and  $a$  is the quantum correction term<sup>11</sup>. And  $s$  is the total number of vibrational degrees of freedom in the molecule.  $I^\ddagger/I$  is the ratio of moment of inertias of the complex and the molecule for degrees of active internal rotations.

According to Whitten-Rabinovitch's formulation<sup>11b,12,13</sup> the general expression for  $\sum P(E_{VR})$  is given by

$$\sum P(E_{VR}) = \frac{P_R(E + aE_z)^{r+1/2}}{(kT)^{r+1/2} \Gamma(s+1+r/2) \prod (h\nu_i)} \quad (4)$$

where  $P_R$  is the rotational partition function for  $r$  internal rotations. And  $N(E_V)$  becomes

$$N(E_V) = \frac{\partial \sum P(E_V)}{\partial E} = \frac{(E + aE_z)^{r-1} \left[ 1 - \beta \left( \frac{dw}{dx} \right) \right]}{\Gamma(s) \prod (h\nu_i)} \quad (5)$$

where  $\beta$  has been termed a frequency dispersion parameter.

Upon making use of eqs. 1-5, the reduced rate constant,  $k_{\text{uni}}/k_\infty$  is expressed as eq. 6

$$G_2(x) = \left[ x + 1 - \frac{\beta^\ddagger}{b_3 x + b_4 x^{b_5} + b_6} \right] \alpha^\ddagger, \quad \theta \leq x \leq 1.0$$

$$G_3(x) = \left[ x + 1 - \beta^\ddagger \exp(-b_1 x^{b_2}) \right] \alpha^\ddagger, \quad 1.0 \leq x \leq 8.0$$

$$H(x) = \left\{ x + \frac{E_c}{E_z^\ddagger} + \frac{E_z}{E_z^\ddagger} \left[ 1 - \beta \exp\left(-b_1 \left(\frac{E_z^\ddagger}{E_z}\right)^{b_2}\right) \right] \right. \\ \left. \left( -\frac{E_c}{E_z} + x \right)^{b_1} \right\}^\alpha$$

$$A_2 = \frac{(E_z^\ddagger)^{\alpha^\ddagger - \alpha}}{2h(RT)^{(r+1)/2}} \left( \frac{\sigma_1^\ddagger}{\sigma_1} \right) \left( \frac{P_R^\ddagger}{P_R} \right)$$

$$\frac{\Gamma(\alpha^\ddagger + 1) \prod_{i=1}^s h\nu_i}{\Gamma(\alpha^\ddagger + 1) \prod_{i=1}^s h\nu_i^\ddagger}$$

$$A_1 = \frac{(E_c^\ddagger)^{\alpha^\ddagger + 1}}{P_V^\ddagger (RT)^{r+1/2} \Gamma(\alpha^\ddagger + 1) \prod_{i=1}^s h\nu_i^\ddagger}$$

and  $\alpha, \alpha^\ddagger$  are defined as

$$\alpha = s + r/2 - 1$$

$$\alpha^\ddagger = s^\ddagger + r^\ddagger/2$$

TABLE 1: Molecular Parameters for Molecule and Activated Complex

	Molecule	Comple
	Geometrical	Parameter
$r_{C-C}$	1.518 Å	1.412 Å
$r_{C-Br}$	1.950 Å	2.131 Å
$r_{C-H(\text{methylene})}$	1.087 Å	1.087 Å
$r_{C-H(\text{methyl})}$	1.093 Å	1.093 Å
		1.274 Å
$\angle CCB$	111°2'	88°12'
$\angle HCH(\text{methylene})$	109°54'	109°54'
$\angle CCH(\text{methylene})$	112°15'	112°15'
$\angle HCB$	105°25'	105°25'
$\angle HCH(\text{methyl})$	108°52'	108°52'
$r_{H\cdots Br}$		1.595 Å
$\angle H\cdots Br$		90°
	Moment of Inertia, $10^{-39}$ gcm <sup>2</sup>	
$I_A$	23.7	21.3
$I_B$	22.0	19.1
$I_C$	2.78	3.24

TABLE 2: Input Parameters for RRKM Calculation

Collision diameter	$C_2H_5Br^a$	5.13 Å at 311.4°K
	$C_2H_5Br$ and $CO_2^b$	4.57 Å
Activation energy	53.9 kcal/mole	
	Molecule	Complex
Zero point energy kcal/mole	39.91	35.67
Symmetry number	1	1
Number of internal rotational degrees of freedom	0	0
Number of vibrational degree of freedom	18	17

<sup>a</sup>"Handbook of Chemistry and Physics", 42nd Ed., Chemical Rubber Publishing Co., 1960-1961 pp 2205. <sup>b</sup>J. O. Hirschfelder, C. F. Curtiss and R. B. Bird, "Molecular Theory of Gase and Liquid", John Wiley and Son, Inc., New York, N.Y., 1954 pp.209. S. W. Benson and H. E. O'Neil, "Kinetic Data on Gas Phase Reaction", NSRDS-NBS 21, 1970 pp 89.

and other constants used in eq.8 are listed in Table 4.

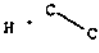
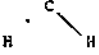
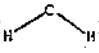
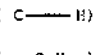
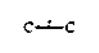





The actual integrations of eq. 8 were carried out with the aid of a CDC Cyber 170 computer, KIST, Seoul.

## Results

The pressure dependence studies in terms of the reduced reaction rate constant were carried out in their fall-off regions at 724.5, 744.5, and 755.1 °K, respectively. These results are tabulated in Table 5. Theoretical plots in this system are given in Figures 1, 2, and 3 together with experimental values for the comparison.

Experimental points are in good agreements with the theoretical curves with the correction of collisional efficiency  $\beta$ . Qualitatively, at high pressures collisional activation prevails over energy redistribution in the molecule and  $\beta$  is almost unity. But at low pressures, energy redistribution prevails over collisional process, so collisional efficiency

TABLE 3: Vibrational Frequencies for Molecule and Activated Complex

Ethyl Bromide, $C_2H_5Br^a$			Activated Complex <sup>b</sup>		
No.	type of mode	frequency (cm <sup>-1</sup> )	type of mode	frequency (cm <sup>-1</sup> )	
$\nu_1$	CH <sub>3</sub> d-stretch	2988		562	
$\nu_2$	CH <sub>2</sub> s-stretch	2937			
$\nu_3$	CH <sub>3</sub> s-stretch	2880		717	
$\nu_4$	CH <sub>2</sub> scis	1451			
$\nu_5$	CH <sub>3</sub> d-deform	1451		1434(2)	
$\nu_6$	CH <sub>3</sub> s-deform	1386		2962(4)	
$\nu_7$	CH <sub>2</sub> wag	1252		2094	
$\nu_8$	CH <sub>3</sub> rock	1061		1181	
$\nu_9$	CC stretch	964		1124(4)	
$\nu_{10}$	CBr stretch	583			
$\nu_{11}$	CCBr deform	290		385	
$\nu_{12}$	CH <sub>2</sub> a-stretch	3018			
$\nu_{13}$	CH <sub>3</sub> d-stretch	2988		400	
$\nu_{14}$	CH <sub>3</sub> d-deform	1451		412	
$\nu_{15}$	CH <sub>2</sub> twist	1248			
$\nu_{16}$	CH <sub>3</sub> rock	964			
$\nu_{17}$	CH <sub>2</sub> rock	770			
$\nu_{18}$	Torsion	247			

<sup>a</sup>T. Shimanouchi, "Tables of Molecular Vibrational Frequencies", Consolidated vol. 1, NSRDS-NBS 39, 1972. <sup>b</sup>S. W. Benson and H. E. O'Neil, "Kinetic Data on Gas Phase Unimolecular Reaction", NSRDS-NBS 21, 1970.  $(\text{---})_2$  indicates the propylene type torsion around a three electron bond.

TABLE 4: List of Empirical Constants<sup>a</sup>

$b_1 = 2.419$
$b_2 = 0.25$
$b_3 = 5.00$
$b_4 = 2.73$
$b_5 = 0.5$
$b_6 = 3.510$

<sup>a</sup>Ref. 11.

plays an important role. In the fall-off region, balance is maintained between intermolecular and intramolecular energy transfer. Quantitatively,  $\beta$  is expressed<sup>15</sup> as the ratio of specific reaction rate constant by substrate-inert gas collision and by substrate-substrate collision at the pressures of equal collision frequencies. In this manner,  $\beta$  is obtained and its value is about 0.4-0.6 for CO<sub>2</sub> at each pressures. For methyl isocyanide isomerization<sup>16</sup>,  $\beta_c$  for CO<sub>2</sub> was 0.55. The discrepancies due to collisional efficiency are more remarkable at low temperatures. The experimental curves could be studied with the present technique only in the fall-off region. Plots of  $k_{uni}$  vs.  $P^{-1}$  give good results of  $k_{\infty}$  values<sup>14</sup> and a typical plot at 744.5 K is given in Figure. 4. Activation energy and Arrhenius A-factor were obtained by the ln k

**TABLE 5: Pressure Dependence of the Reduced Rate Constant Ratio for  $C_2H_5Br-CO_2$  at 724.5–755.1 °K**

at 724.5 °K			at 744.5 °K			at 755.1 °K		
P, Torr	$k \times 10^4, \text{sec}^{-1}$	$k/k_\infty$	P, Torr	$k \times 10^4, \text{sec}^{-1}$	$k/k_\infty$	P, Torr	$k \times 10^4, \text{sec}^{-1}$	$k/k_\infty$
1.90	1.33	0.25	2.23	3.57	0.17	1.38	6.37	0.234
2.64	1.44	0.27	3.18	3.81	0.18	2.18	7.50	0.276
3.78	1.57	0.30	3.69	4.01	0.19	2.20	7.44	0.274
4.65	1.66	0.31	3.83	4.58	0.21	3.01	7.69	0.283
7.62	2.83	0.53	4.70	3.02	0.14	3.56	7.30	0.268
15.24	3.83	0.72	4.86	5.00	0.23	3.74	7.53	0.277
27.94	3.54	0.67	7.33	12.4	0.51	4.46	9.34	0.343
57.91	3.94	0.74	26.63	15.0	0.70	5.44	10.83	0.398
			56.92	18.6	0.84	14.83	15.30	0.563
						29.66	22.92	0.843

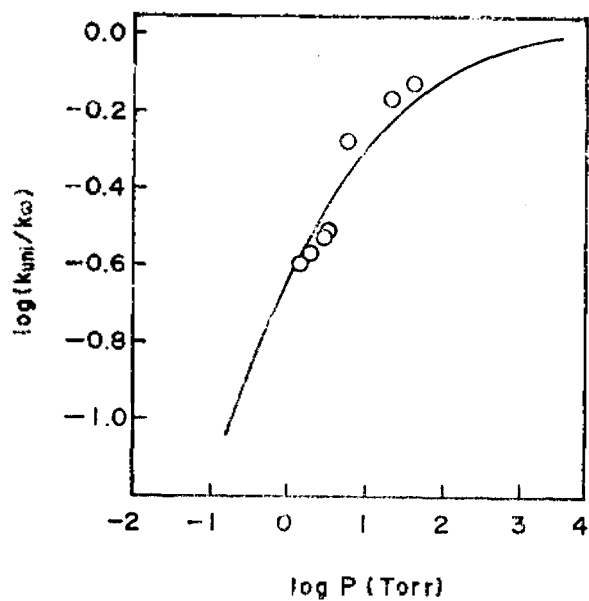
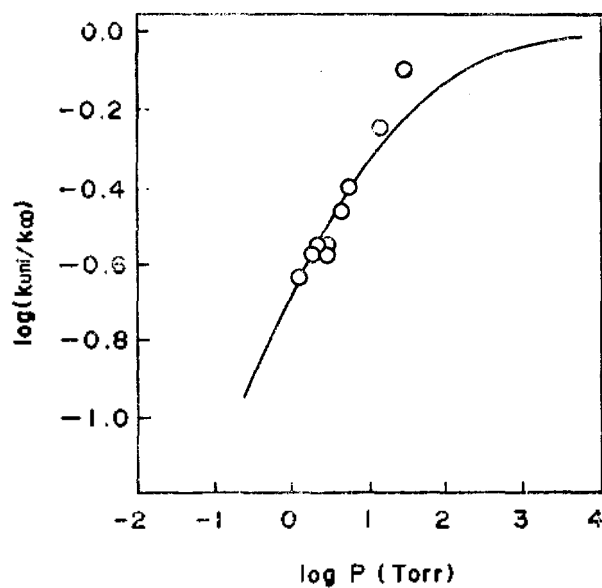
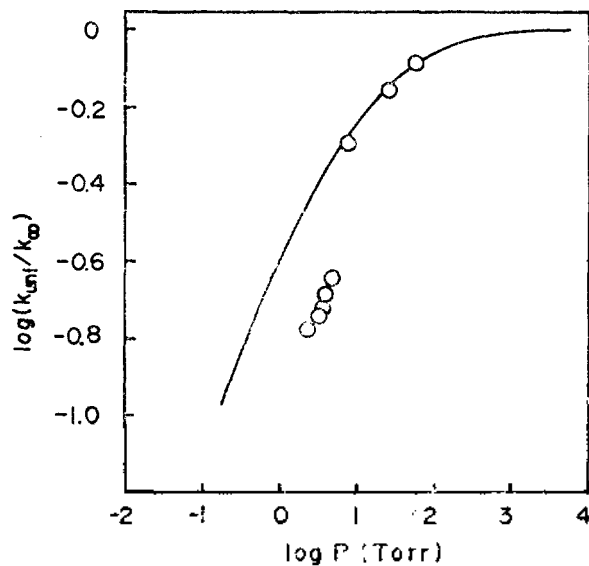
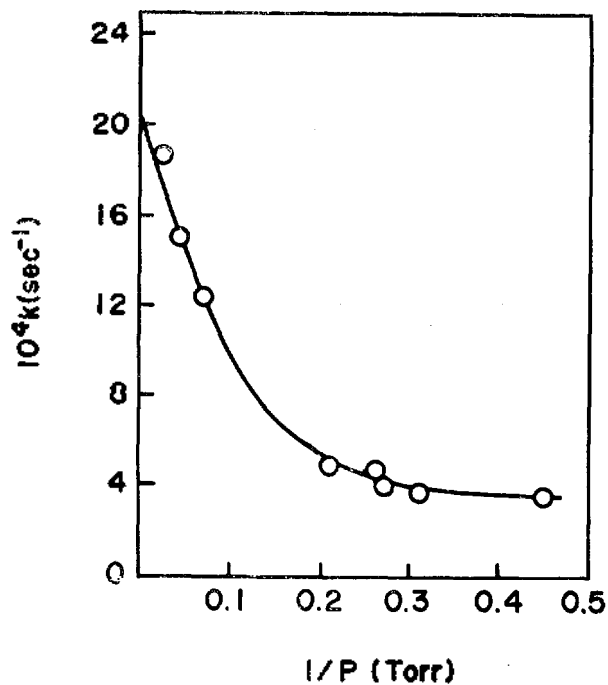

**Figure 1.** Fall-off plot of  $C_2H_5Br$  Thermal Dissociation at 724.5 °K. (—) Theoretical line; (○) Experimental points.

**Figure 3.** Fall-off plot of  $C_2H_5Br$  Thermal Dissociation at 755.1 °K. (—) Theoretical line; (○) Experimental points.

**Figure 2.** Fall-off plot of  $C_2H_5Br$  Thermal Dissociation at 744.5 °K. (—) Theoretical line; (○) Experimental points.

**Figure 4.** Determination of  $K_\infty$  at 744.5 °K.

TABLE 6: Estimated First Order Rate Constants at 724.5 755.1 °K, A-factor and Activation Energy

$k_{\infty}$ , sec <sup>-1</sup>	
at 724.5 °K	$5.3 \times 10^{-4}$
at 744.5 °K	$21.4 \times 10^{-4}$
at 755.1 °K	$27.2 \times 10^{-4}$
A-factor	$10^{12.5} (10^{13.3})^a$
$E_a$ , kcal/mole	51.7 (53.9) <sup>a</sup>

<sup>a</sup>Ref. 4.

vs.  $T^{-1}$  plot. Obtained values of  $k_{\infty}$  at various temperatures,  $E_a$  and A-factor are given in Table 6. They are in relatively good agreements with an earlier worker<sup>4</sup> at high pressures.

## Discussion

The most important foundations for RRKM approach are based on (i) the free exchange of intramolecular energies and (ii) the strong collision assumption. Though some contradictory arguments arose time to time<sup>17,18</sup>, the rapid energy (i) between all vibrational modes of the molecules during their lifetimes for particularly not so large molecules are proven to have universal acceptance among workers<sup>17,19</sup>. The strong collision assumption (ii) anticipates that the relatively large amounts of energy (usually  $\gg RT$ ) are transferred in molecular collisions. It is generally accepted that this assumption is reasonably realistic for thermal reactions in the temperature range of conventional kinetic studies of moderate size molecules. The choice of  $C_2H_5Br$  and the temperature range we studied are thought to be adequate for RRKM treatment on the basis of foregoing discussion.

Studies<sup>16</sup> of the energizing efficiencies of various gases in the second-order region show that collisional efficiencies,  $\beta$ , are within a factor of ten and a limiting efficiency for molecules above a certain moderate size is presumed to be unity. Therefore, pressure fall-off curve is shifted to higher pressures by an increment  $\log \beta$ . In theoretical fall-off curves, Figures 1, 2, and 3, the fact that curves with added  $CO_2$  gas are always higher than those of ethyl bromide indicates that collisional efficiency of  $CO_2$  is for smaller than that of ethyl bromide.

Since our experiments were carried out only in the fall-off region, generally designated to be  $10^{-1}$ – $10^2$  torr, plots of  $k$  vs.  $1/P$  were made to obtain the value of  $k_{\infty}$ <sup>14</sup>.

The fact that the experimentally obtained Arrhenius A-factor is less than  $10^{13}$  means that there are no free internal rotations and bond ruptures of C-C and C-Br are not reaction coordinates. And since  $\Delta S_{exp}$  is negative, ca.  $-7$  e.u., it was suggested that there should exist a tight activated complex. Mechanism of four-center elimination was also supported.

In order to obtain the geometry of the activated complex proposed previously, an optimization may be performed using the MO theory, but it is not appropriate since no such techniques which can be applied for d-electron systems are available at present time. Thus we have adopted a semiempirical method, i.e., Bond-Energy-Bond-Order (BEBO)

method<sup>20</sup> as an alternative choice. Partial bond orders for C-C, C-Br, Br-H and H-C were assumed to be 1.5, 0.5, 0.5 and 0.5, respectively. With the use of Pauling's Equation<sup>21</sup> and partial bond orders, bond lengths were obtained. Seven models of the complex were assumed by varying CCB<sub>r</sub> and CCH angles and the principal moment of inertia for each model was calculated. Out of these, we have chosen one which had the largest value of the moment of inertia since it minimizes the rotational energy.

Frequencies of the molecule were obtained from the experimental data<sup>22</sup>. Though for the activated complex frequency assignment could be accomplished by the normal coordinate analysis, Benson's method which uses the Badger's rule<sup>23</sup> was adopted in this study because the normal coordinate analysis was unnecessarily complicate and the obtained data by Benson for various systems were in good agreement with experimental values.<sup>24</sup>

Torsional vibration of the reactant molecule was designated as the reaction coordinate since reaction occurs through the torsional vibration.

There are several methods obtaining the density of energy states. Among these, the direct counting of energy levels is the most accurate one of all, but very time-consuming even for a small size of molecule. Since experiments were carried out only in the fall-off region, it was not necessary for the precise comparison between theory and experiment to be made throughout the entire range and it may be adequate with a simple approximation technique such as Whitten-Rabinovitch approximation<sup>11, 12, 13</sup>.

In the numerical integration, centrifugal correction factor,  $F_w$ , was assumed to be unity and collision cross section,  $\sigma$ , obtained from viscosity data<sup>23</sup>, was somewhat uncertain. Therefore, theoretical fall-off curves were expected to be slightly overestimated.

Although the sparsity of data points at both high pressure and low pressure regions and the introduction of an arbitrary parameter, e.g.,  $\beta$ , make it difficult to draw definite conclusions, it appears that the kinetic data support the complex model we assumed in this study and the validity of the RRKM theory for the prediction of the fall-off behavior.

## Conclusions

Considering that the predicted fall-off curve of this system with introducing an arbitrary collision parameter, e.g.,  $\beta$ , shows satisfactory agreement with kinetic data, a tight activated complex model with "tight" ordinary vibrations appears to be reasonable for the  $C_2H_5Br$  unimolecular decomposition reaction. Conversely, this agreement can be taken as an evidence of the validity of the RRKM formulation for the prediction of the fall-off behavior.

Although the calculated fall-off curve shows some quantitative agreement with  $C_2H_5Br$  data, the introduction of parameter makes some desires for further development along the line of theoretical approach as well as the ample accumulation of experimental data.

*Acknowledgement.* Funds from the Korea Research Center

for Theoretical Physics and Chemistry were greatly appreciated. One of the authors (K. H. Jung) wishes to express his appreciation to Professor Mu Shik Jhon for his contribution to the computation of this project.

### References

- (1) P. Fugassi and F. Daniels, *J. Amer. Chem. Soc.*, **60**, 771 (1938).
- (2) A. T. Blades and G. W. Murphy, *J. Amer. Chem. Soc.*, **74**, 6219 (1952).
- (3) A. E. Goldberg and F. Daniels, *J. Amer. Chem. Soc.*, **79**, 1314 (1957).
- (4) P. J. Thomas, *J. Chem. Soc.*, 1192 (1959).
- (5) (a) R. A. Marcus and O. K. Rice, *J. Phys. and Colloid Chem.*, **55**, 894 (1951); (b) R. A. Marcus, *J. Chem. Phys.*, **20**, 359 (1952); (c) G. M. Wieder and R. A. Marcus, *J. Chem. Phys.*, **37**, 1835 (1962).
- (6) R. A. Marcus, *J. Chem. Phys.*, **43**, 2658 (1965).
- (7) E. V. Waage and B. S. Rabinovitch, *J. Chem. Phys.*, 5581 (1970).
- (8) E. V. Waage and B. S. Rabinovitch, *Chem. Rev.*, **70**, 377 (1970).
- (9) A. J. Hay and R. L. Belford, *J. Chem. Phys.*, **47**, 3944 (1967).
- (10) W. Forst, *J. Chem. Phys.*, **48**, 3665 (1968).
- (11) (a) B. S. Rabinovitch and J. H. Current, *J. Chem. Phys.*, **35**, 2250 (1961); (b) G. Z. Whitten and B. S. Rabinovitch, *J. Chem. Phys.*, **38**, 2466 (1963); (c) G. Z. Whitten and B. S. Rabinovitch, *J. Chem. Phys.*, **41**, 1883 (1964).
- (12) B. S. Rabinovitch and R. W. Diesen, *J. Chem. Phys.*, **30**, 735 (1959).
- (13) B. S. Rabinovitch and D. W. Setser, *Advan. Photochem.*, **3**, 1 (1964).
- (14) E. Tschuikow-Roux, K. O. MacFadden, K-H. Jung and D. A. Armstrong, *J. Phys. Chem.*, **77**, 734 (1973).
- (15) D. C. Tardy and B. S. Rabinovitch, *J. Chem. Phys.*, **48**, 1282 (1968).
- (16) S. C. Chan, B. S. Rabinovitch, J. T. Bryant, L. D. Spicer, T. Fujimoto, Y. N. Lin and S. P. Pavlou, *J. Phys. Chem.*, **74**, 3160 (1970).
- (17) (a) J. D. Rynbrandt and B. S. Rabinovitch, *J. Phys. Chem.*, **74**, 4175 (1970); (b) *ibid.*, **75**, 2164 (1971).
- (18) D. L. Bunker, "Theory of Elementary Gas Reaction Rates", Pergamon Press, Oxford, 1966.
- (19) J. N. Butler and G. B. Kistiakowsky, *J. Amer. Chem. Soc.*, **82**, 759 (1960).
- (20) H. S. Johnston, "Gas Phase Reaction Rate Theory", Ronald Press, New York, 1966.
- (21) L. Pauling, "The Nature of the Chemical Bond", 3rd Ed., Cornell University Press, Ithaca, 1960, pp. 225.
- (22) T. Shimanouchi, "Tables of Molecular Vibrational Frequencies", Consolidated vol. 1, NSRDS-NBS 39, 1972, pp. 105.
- (23) (a) H. S. Johnston and P. Goldfinger, *J. Chem. Phys.*, **37**, 700 (1962); (b) H. S. Johnston and C. Parr, *J. Amer. Chem. Soc.*, **85**, 2544 (1963).
- (24) S. W. Benson and H. E. O'Neil, "Kinetic Data on Gas Phase Unimolecular Reactions", NSRDS-NBS 21, 1970.
- (25) Handbook of Chemistry and Physics, 42nd Ed., Chemical Rubber Publishing Co., 1960-1961.

## Vacuum Ultraviolet Photolysis of Ethyl Bromide at 123.6nm

Hee Soo Yoo and K. H. Jung

Department of Chemistry, Korea Advanced Institute of Science, Seoul 131, Korea (Received March 13, 1980)

A vacuum ultraviolet photolysis of ethyl bromide was studied in the pressure range of 0.5-19.9 torr and at 123.6 nm krypton resonance line. The pressure effect on the reaction was studied by increasing the reactant pressure and by adding an inert gas, e.g., He. In the observation the monatomic gas is found to be no effect in the reaction. A scavenger effect of the reaction was also performed by adding NO gas as a radical scavenger and was found to be quite efficient to scavenge a radical product C<sub>2</sub>H<sub>5</sub>. The observation of the major reaction product C<sub>2</sub>H<sub>6</sub> was interpreted in terms of a molecular elimination. Nonetheless the decreasing phenomenon of  $\phi_{C_2H_5}/\phi_{C_2H_4}$  with pressure rise was attributed to the existence of the two electronically excited states. One state proceeds to the molecular elimination and the other to carbon-bromine bond fission. The excitation and the decomposition mechanisms between two excited states and the reaction products were interpreted in terms of the first excitation which proceeds the molecular elimination, and the second excitation which resulted from the first excited state by collisional cross over decomposes by carbon-bromine bond fission.

### Introduction

Recent studies on the vacuum ultraviolet photolyses of ethylhalides have shown many possible primary processes<sup>1-9</sup>

often competing the molecular elimination with the radical formation. In general, alkyl halides dissociate to alkyl radicals and halogen atoms when alkyl halides are irradiated within the first absorption band, while they proceed the molecular